Supporting Information

Polyphenolic Oligomer-Derived Multienzyme Activity for Treatment of Ischemic Stroke through ROS Scavenging and Blood-Brain Barrier Restoration

Wei Meng,[a,b] Zhifang Ma,[a]* Hongbo Ye,[a] Lei Liu,[a,b] Qiaoyi Han[a,b], Qiang Shi,[a,b,c]*

a. State Key Laboratory of Polymer Physics and Chemistry, Changchun Institute of Applied Chemistry, Chinese Academy of Sciences, Changchun, Jilin 130022, China

b. School of Applied Chemistry and Engineering, University of Science and Technology of China, Hefei 230026, China

c. Key Laboratory of Polymeric Materials Design and Synthesis for Biomedical Function, Soochow University, Suzhou, Jiangsu 215123, China

* Corresponding authors

Email: shiqiang@ciac.ac.cn, zfma@ciac.ac.cn

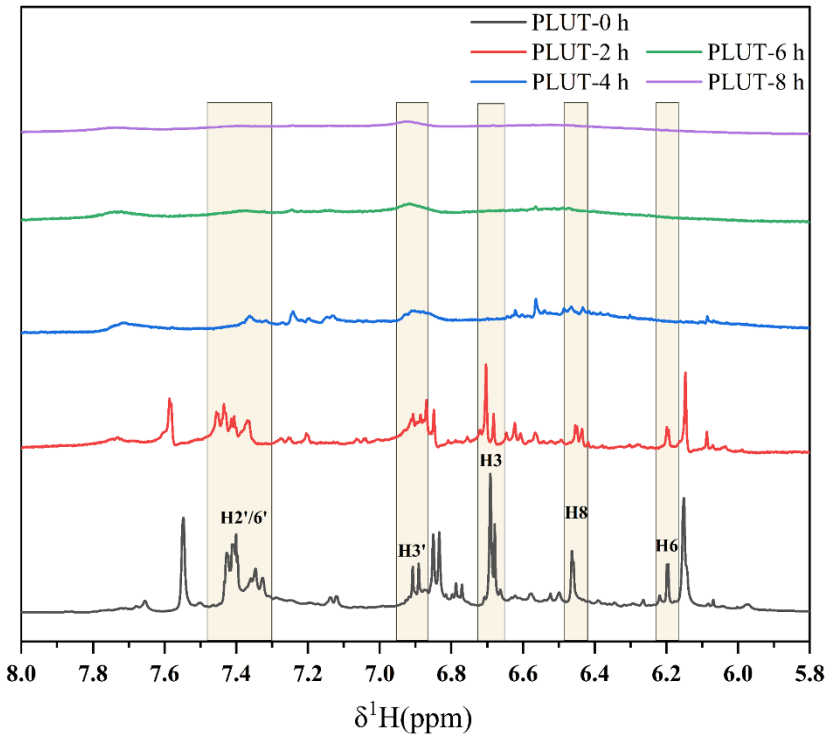

Fig. S1. ^{1}H NMR spectra of PLUT2 under hydrothermal conditions at different point-in-time of 0, 2, 4, 6, and 8 h.

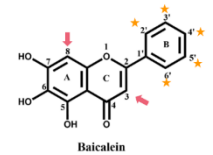

	H3	H8	Ar-CH2-C	Ar-CH2-Ar
PBAI1	0.86±0.04	0.26±0.02	0.18±0.05	0.25±0.01
PBAI2	0.65±0.03	0.17±0.03	0.42±0.03	0.42±0.02

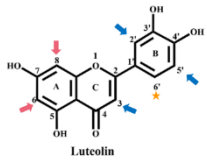

	H3	H6	H8	H2′	H5′	Ar-CH2-C	Ar-CH2-Ar
PLUT1	0.82±0.02	0.31±0.02	0.41±0.01	0.66±0.02	0.51±0.05	0.94±0.04	0.98±0.08
PLUT2	0.5±0.01	0.13±0.01	0.25±0.03	0.58±0.02	0.58±0.04	1.02±0.08	1.01±0.04

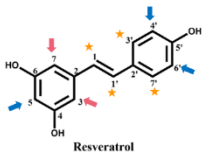

	H3	H5	H7	H4′	H6′	Ar-CH2-Ar
PRES1	0.31±0.01	0.25±0.02	0.31±0.01	0.34±0.02	0.34±0.02	0.16±0.02
PRES2	0.16±0.01	0.23±0.01	0.16±0.01	0.27±0.01	0.27±0.01	0.28±0.04

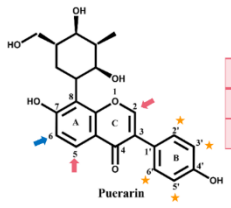

	H2	H5	H6	Ar-CH2-C	Ar-CH2-Ar
PPUE1	0.94±0.02	0.96±0.02	0.98±0.02	0.9±0.09	0.9±0.1
PPUE2	0.89±0.01	0.89±0.01	0.93±0.01	1.1±0.05	1.02±0.03

Table S1. Quantitative analysis of reaction hydrogen from different PPNs in ^{1}H NMR spectra. (The main position was labeled with a red arrow, the minor position was labeled with a blue arrow, and the nonreactive position was labeled with a star.)

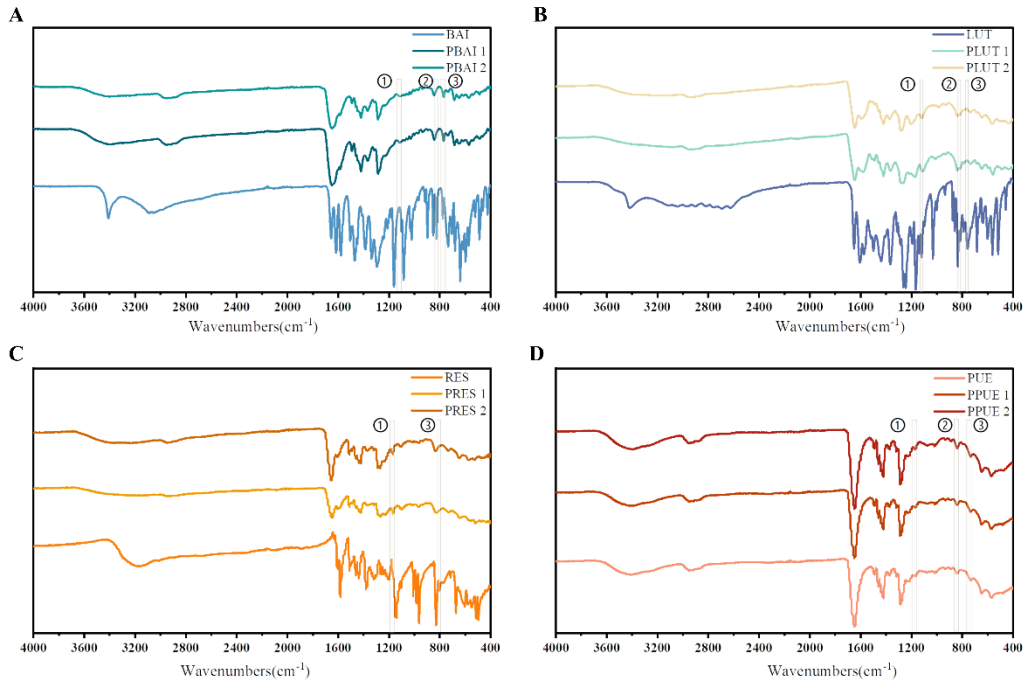

Fig. S2. (A) FT-IR spectra of PBAI and pure BAI (①: 1105(C-O-C); ②: 825(C=C); ③: 776(Ar-H)). (B) FT-IR spectra of PLUT and pure LUT (①: 1120(C-O-C); ②: 816(C=C); ③: 758(Ar-H)). (C) FT-IR spectra of PRES and pure RES (①: 1168(C-O-C); ③: 802(Ar-H)). (D) FT-IR spectra of PPUE and pure PUE (①: 1174(C-O-C); ②: 834(C=C); ③: 747(Ar-H)).

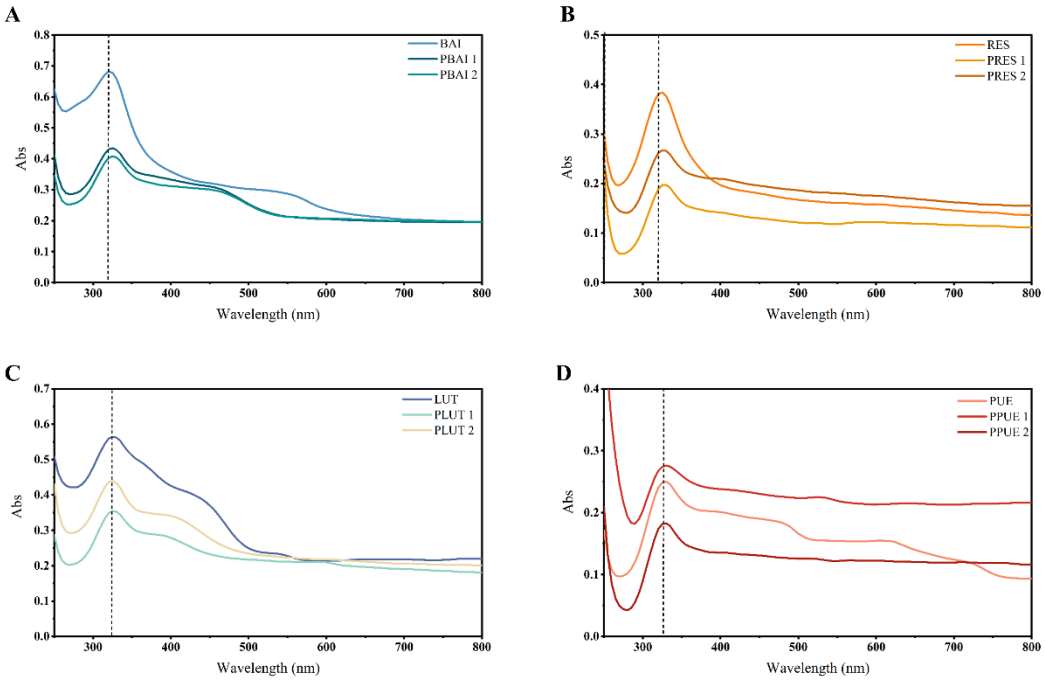

Fig. S3. (A) UV−vis spectra of PBAI and pure BAI. (B) UV−vis spectra of PLUT and pure LUT. (C) UV−vis spectra of PRES and pure RES. (D) UV−vis spectra of PPUE and pure PUE.

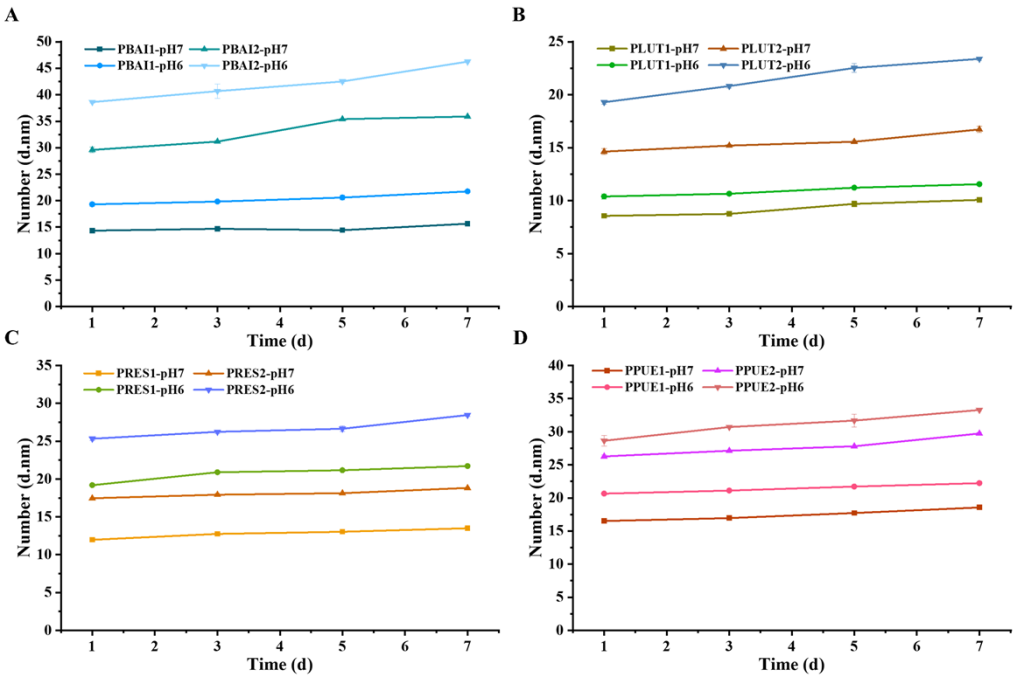

Fig. S4. Size stability of PPN at different pH conditions. (A) Particle size changes of PBAI1 and PBAI2 at pH=6 and 7. (B) Particle size changes of PLUT1 and PLUT2 at pH=6 and 7. (C) Particle size changes of PRES1 and PRES2 at pH=6 and 7. (D) Particle size changes of PPUE1 and PPUE2 at pH=6 and 7.

	PBAI1	PBAI2	PLUT1	PLUT2	PRES1	PRES2	PPUE1	PPUE2
ζ-Potential	-26.56±0.71	-20.20±0.62	-19.83±0.15	-16.33±0.56	-14.76±0.25	-10.56±0.25	-10.81±0.93	-7.67±0.79
Production yield	87.50±3.58	86.85±0.89	86.03±0.92	84.47±3.39	87.94±2.15	88.79±2.81	38.22±3.22	44.03±4.99

Diameter/Day	PBAI1	PBAI2	PLUT1	PLUT2	PRES1	PRES2	PPUE1	PPUE2
1	10.21±2.10	31.40±0.21	5.67±1.16	11.80±2.40	8.70±1.55	22.72±2.40	14.61±1.55	26.32±2.68
3	13.50±0.08	33.10±1.76	7.01±0.72	7.532±2.40	8.70±1.55	19.61±1.97	16.95±1.76	22.72±2.68
5	14.61±1.55	30.41±1.76	4.9±1.04	8.72	10.11±1.55	22.72±2.40	16.95±1.76	26.32±2.68
7	16.95±1.76	29.50	5.67±1.16	7.53±1.56	11.70±0.21	26.32±2.68	14.61±1.55	30.45±3.18

Table S2. Quantitative analysis of diameter, ζ potential, and production yield of PPN.

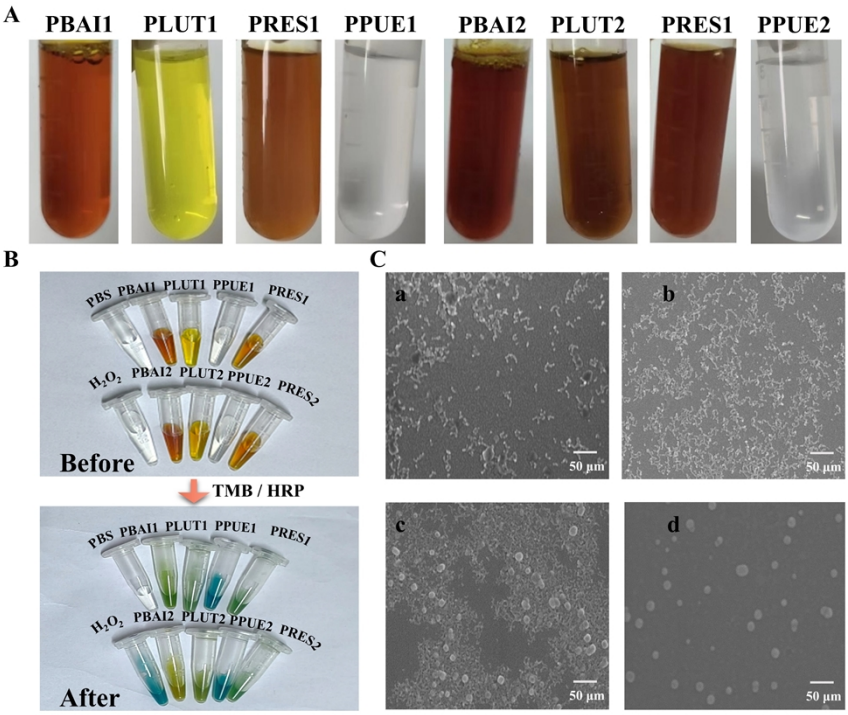

Fig. S5. (A) Color and clarity of the PPN. (B) Photograph of TMB+•OH after incubation with PPN (1 mg/mL). (C) SEM images of intermediates in the formation of PBAI at 1, 5, 7, and 24 h.

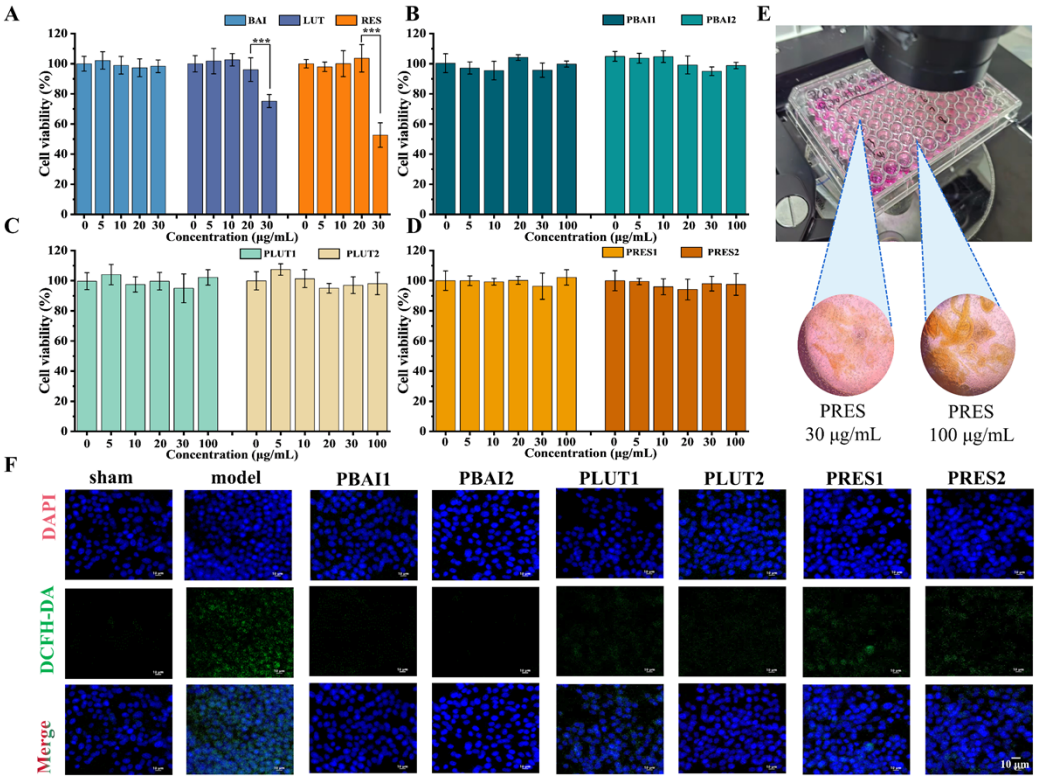

Fig. S6. (A) Viability of PC12 cells incubated with different concentrations of polyphenols (BAI, LUT, and RES). (B) Cell viability of PC12 cells incubated with

different concentrations of PBAI1 and PBAI2. (C) Cell viability of PC12 cells incubated with different concentrations of PLUT1 and PLUT2. (D) Cell viability of PC12 cells incubated with different concentrations of PRES1 and PRES2. (E) Stability of PRES in DMEM medium. (F) Representative images of intracellular ROS levels measured using DCFH-DA after OGD/R in PC12 cells within an optimum concentration of 100 ug/mL of PPN. (Scale bar = 10 μm, ***$p < 0.001$)

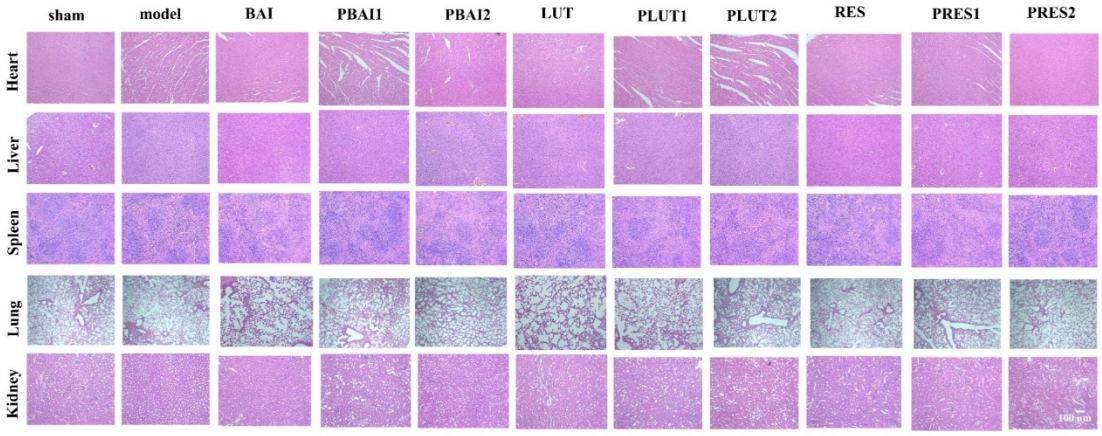

Fig. S7. HE staining of heart, liver, spleen, lung, and kidney after BCCAO/R with the 20 mg/kg injection dose. Scale bar = 100 μm.

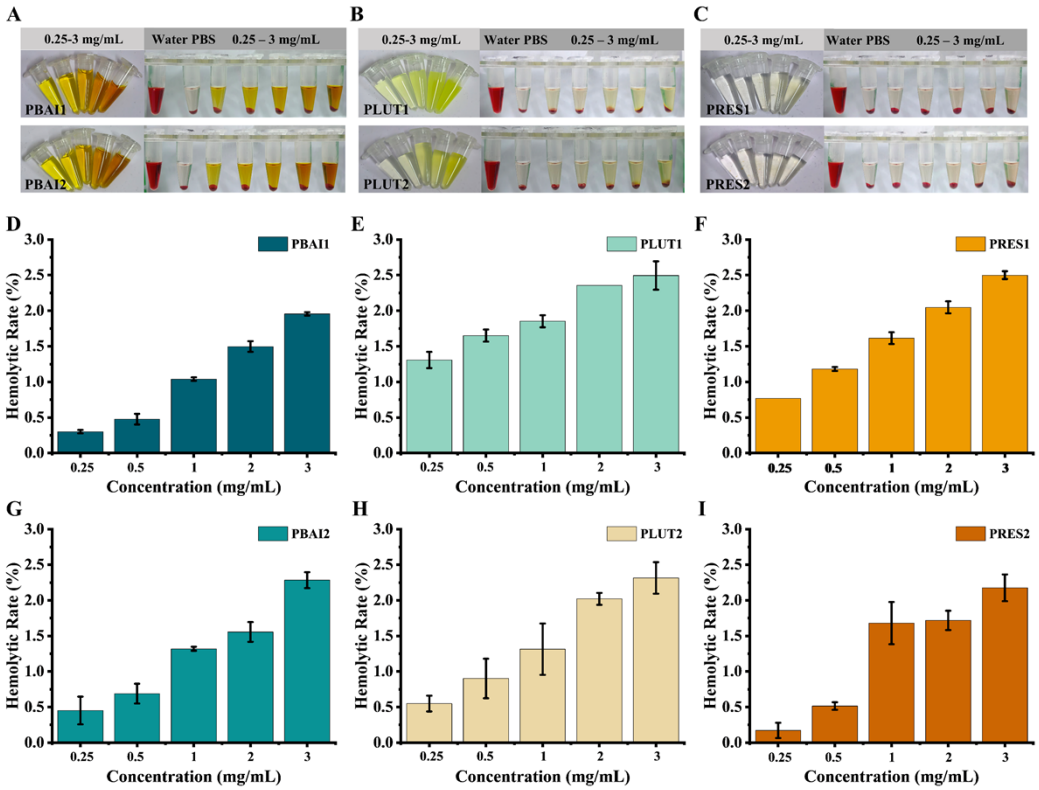

Fig. S8. Biosafety assessment of PPN. (A-C) Photograph of PPN before and after interaction with red blood cells. (D-I) Quantitative analysis of hemolysis rate of PPN.

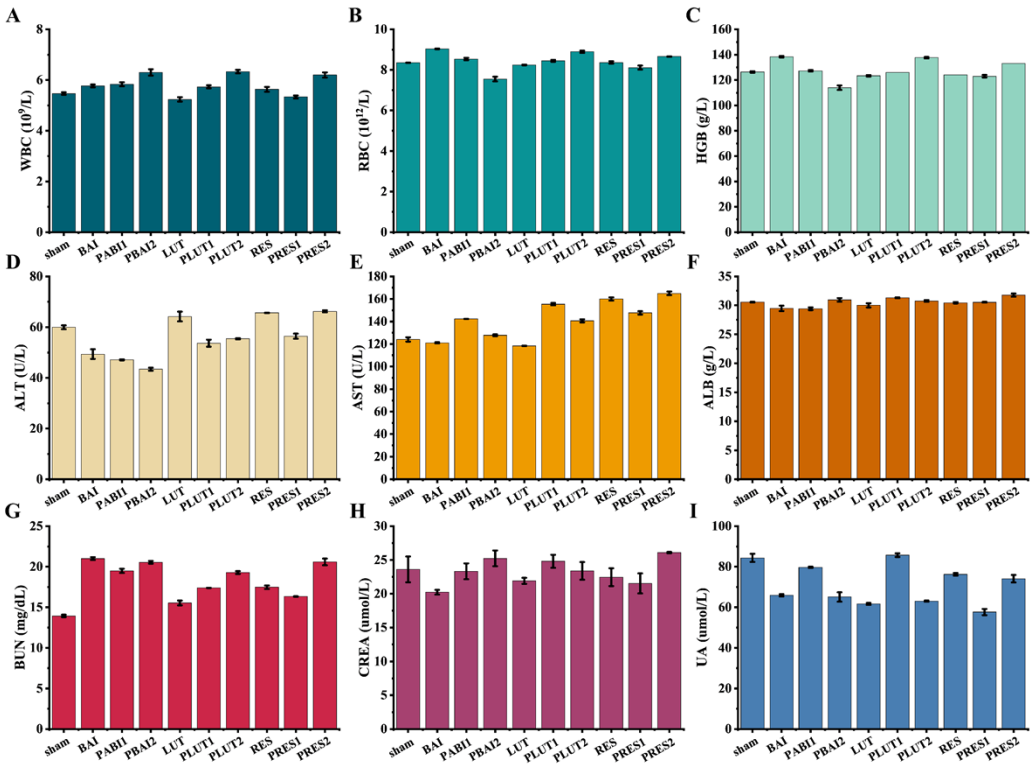

Fig. S9. Vivo metabolic assessment of PPN. Blood test parameters regarding (A) white blood cells (WBC), (B) red blood cells (RBC), and (C) hemoglobin (HGB). Serum levels of liver function indicators: (D) aspartate transaminase (ALT), (E) alanine transaminase (AST), and (F) albumin (ALB). Serum levels of kidney function indicators: (G) blood urea nitrogen (BUN), (H) creatinine (CREA), and (I) uric acid (UA). (the dose was 20 mg/kg, n = 3).

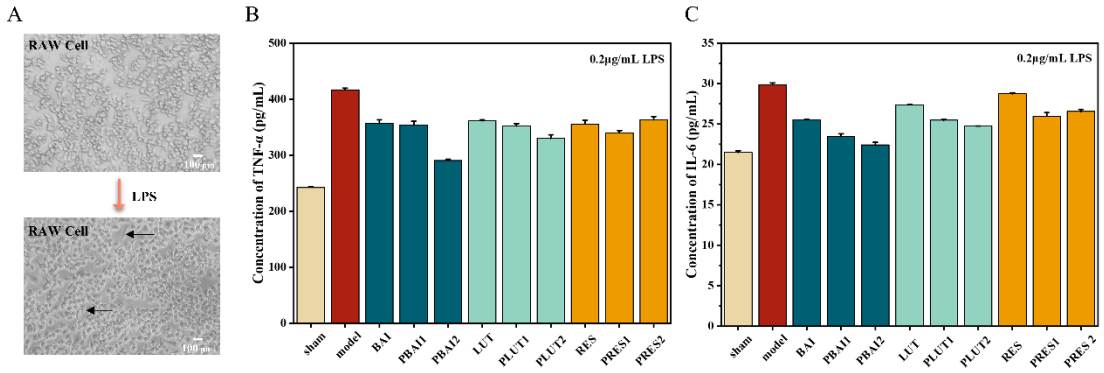

Fig. S10. (A) The morphological changes of RAW cell polarization induced by LPS. (B) Inflammatory factor TNF-α in RAW cells stimulated by LPS (0.2 ug/mL) was examined by ELISA (n = 5). (C) Inflammatory factor IL-6 in RAW cells stimulated by LPS (0.2 ug/mL) was examined by ELISA (n = 5).

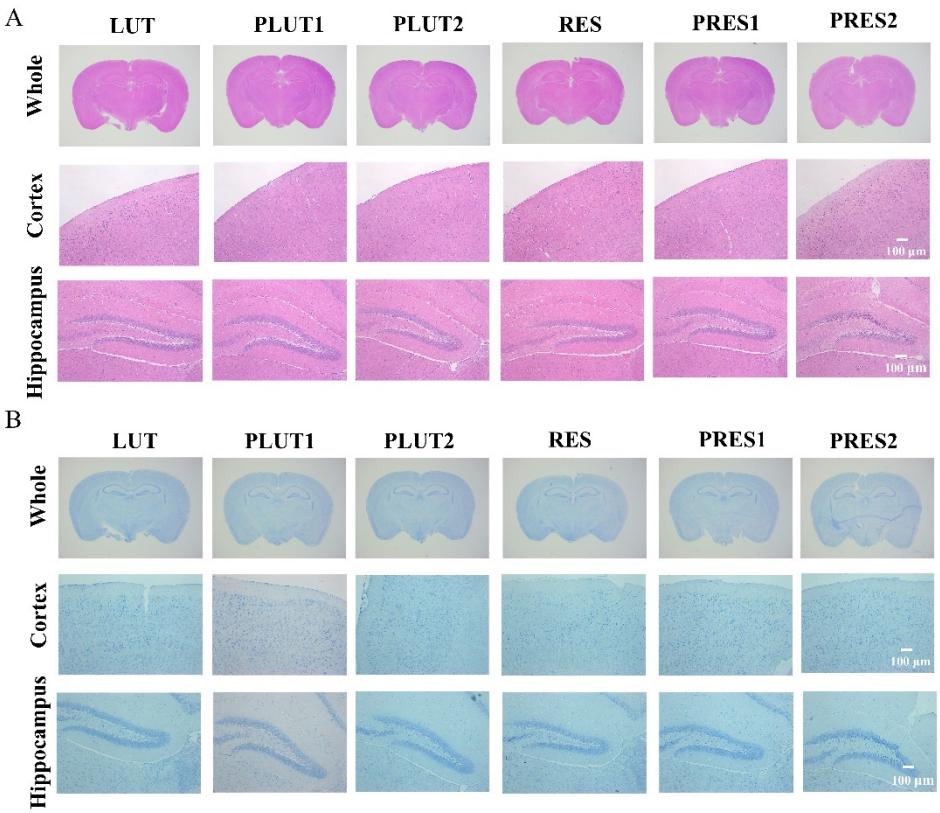

Fig. S11. (A) HE staining of brain sections was used to estimate the morphology of neurons in the whole brain, cortex, and hippocampal region from LUT, PLUT, RES, and PRES treatment. (B) Representative photomicrographs of Nissl staining of brain sections from different treatments from LUT, PLUT, RES, and PRES treatment. (Whole brain: Scale bar = 400 μm; Cortex and hippocampal region: Scale bar = 100 μm)

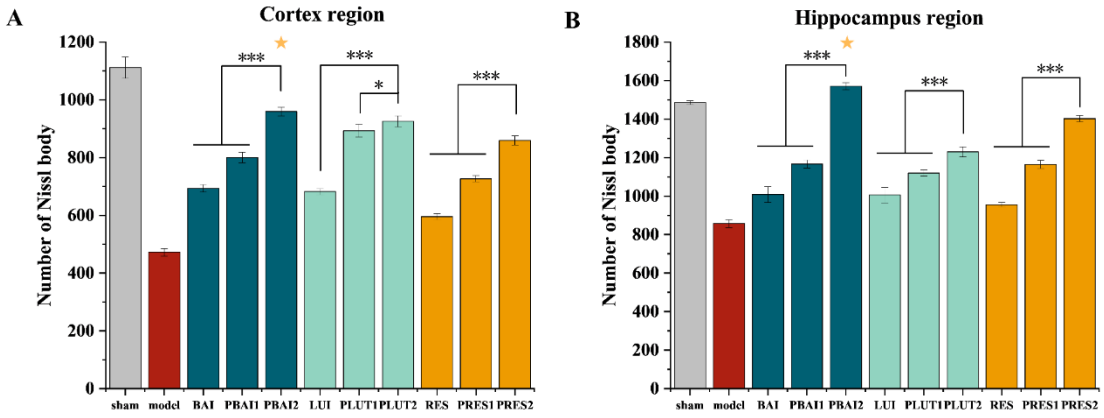

Fig. S12. (A) Quantification of the number of Nissl bodies in cortex neurons. (B) Quantification of the number of Nissl bodies in hippocampus neurons. (n = 5, Star symbol: The treatment group with the highest number of Nissl bodies)

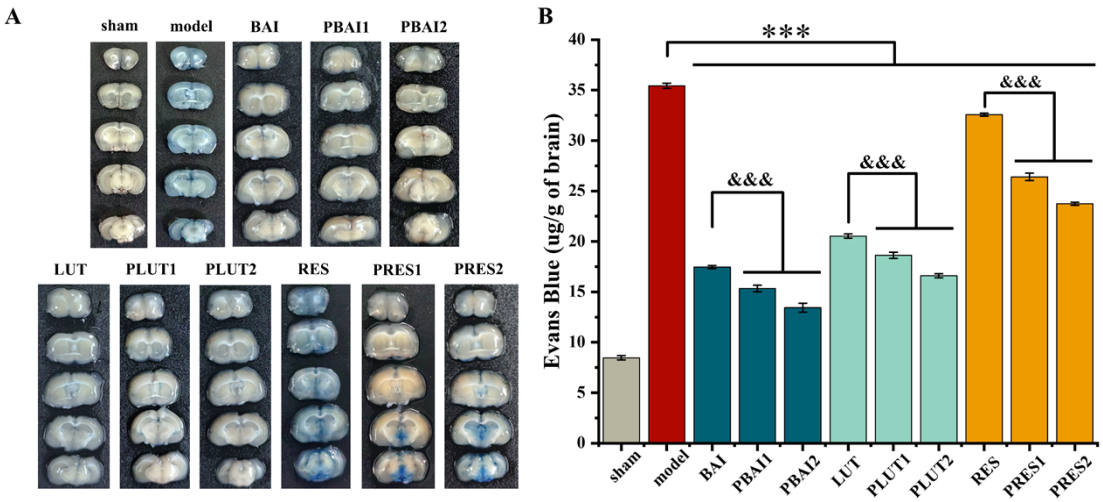

Fig. S13. The BBB repairment of PPN. (A) Representative images of EB-stained brain sections after BCCAO/R. (B) Quantitative analysis of EB content in the whole brain (the dose was 20 mg/kg, n = 5).

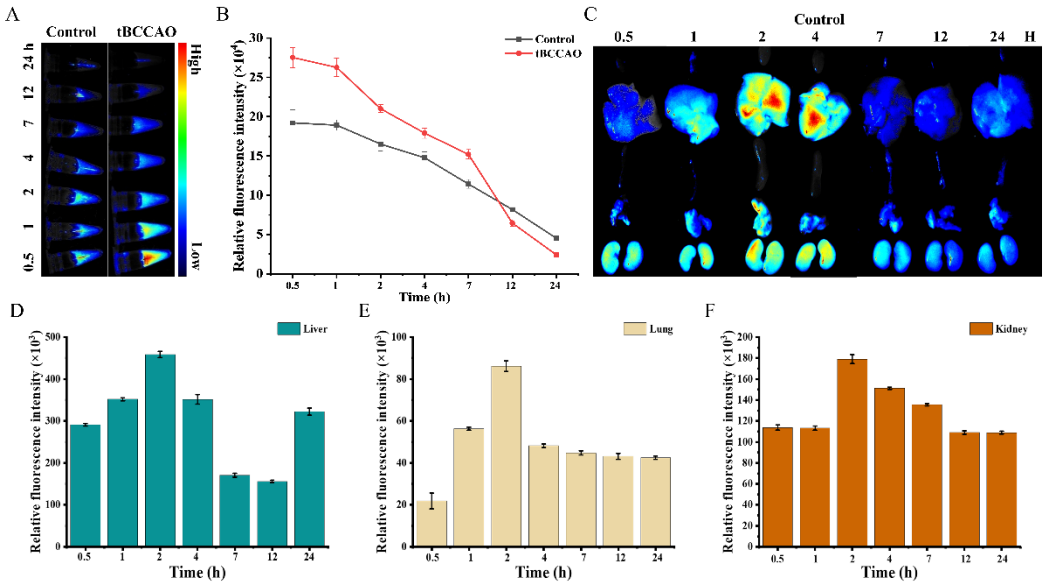

Fig. S14. (A-B) Fluorescence imaging and quantitative analysis of accumulated Cy5-labeled PBAI2 (20 mg/kg) in blood after BCCAO/R at 0.5, 1, 2, 4, 7, 12, and 24 h. Normal animals served as the control group (n=3). (C-F) Fluorescence imaging and quantitative analysis of Cy5-PBAI2 in organs at 0.5, 1, 2, 4, 7, 12, and 24 h in normal health mice.

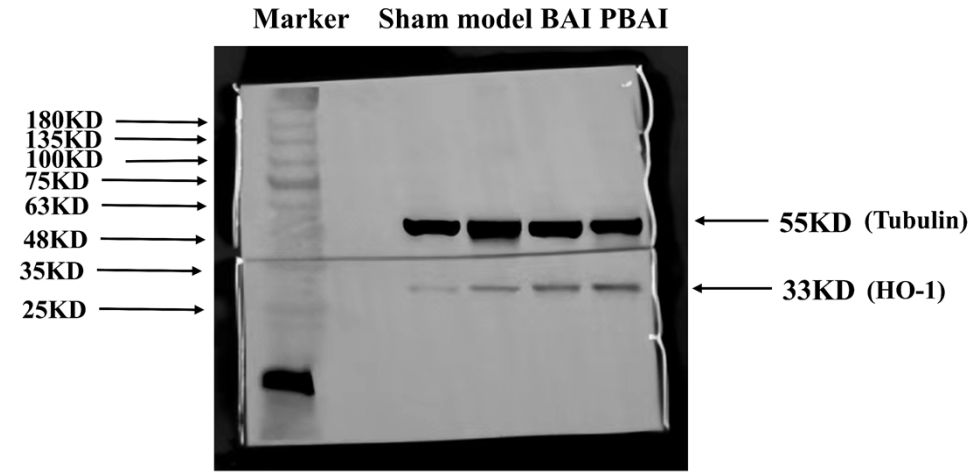

Fig. S15. Protein expression of HO-1 in brain, representative Western blots are presented.

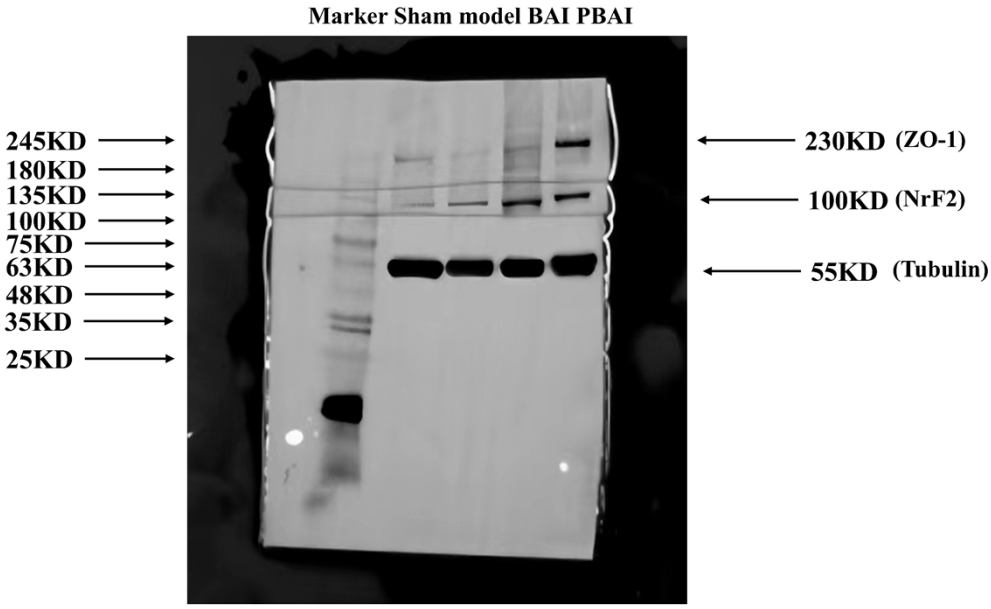

Fig. S16. Protein expression of ZO-1, NrF2 in brain, representative Western blots are presented.

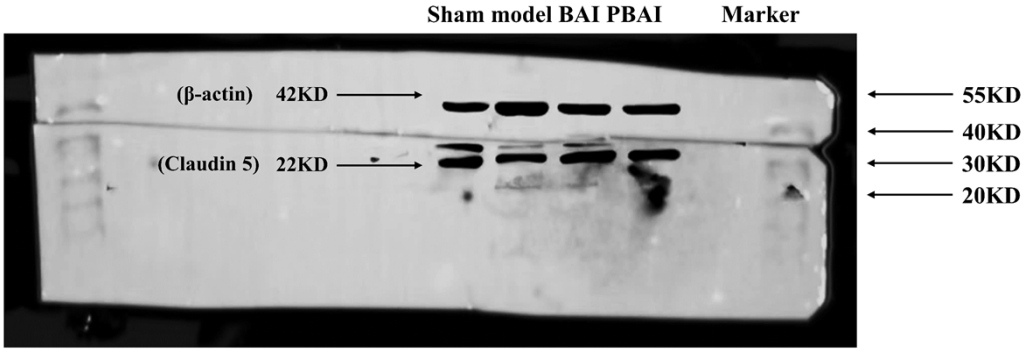

Fig. S17. Protein expression of Claudin5 in brain, representative Western blots are presented.